

High-Level Features Parallelization for Inference Cost Reduction Through Selective Attention

Andre Peter Kelm, Lucas Schmidt, Tim Rolff, Christian Wilms, Ehsan Yaghoubi, Simone Frintrop
Universität Hamburg
Hamburg, Germany

andre.kelm@, lucas.schmidt-1@studium., tim.rolff@, wilms@informatik., ehsan.yaghoubi@,
simone.frintrop@uni-hamburg.de

Abstract

In this work, we parallelize high-level features in deep networks to selectively skip or select class-specific features to reduce inference costs. This challenges most deep learning methods due to their limited ability to efficiently and effectively focus on selected class-specific features without retraining. We propose a serial-parallel hybrid architecture with serial generic low-level features and parallel high-level features. This accounts for the fact that many high-level features are class-specific rather than generic, and has connections to recent neuroscientific findings that observe spatially and contextually separated neural activations in the human brain. Our approach provides the unique functionality of cutouts: selecting parts of the network to focus on only relevant subsets of classes without requiring retraining. High performance is maintained, but the cost of inference can be significantly reduced. In some of our examples, up to 75% of parameters are skipped and 35% fewer GMACs (Giga multiply-accumulate) operations are used as the approach adapts to a change in task complexity. This is important for mobile, industrial, and robotic applications where reducing the number of parameters, the computational complexity, and thus the power consumption can be paramount. Another unique functionality is that it allows processing to be directly influenced by enhancing or inhibiting high-level class-specific features, similar to the mechanism of selective attention in the human brain. This can be relevant for cross-modal applications, the use of semantic prior knowledge, and/or context-aware processing.

1. Introduction

One of the superior capabilities of the human brain is the ability to focus and accelerate processing when high-level knowledge is available. If we search a book in the book-

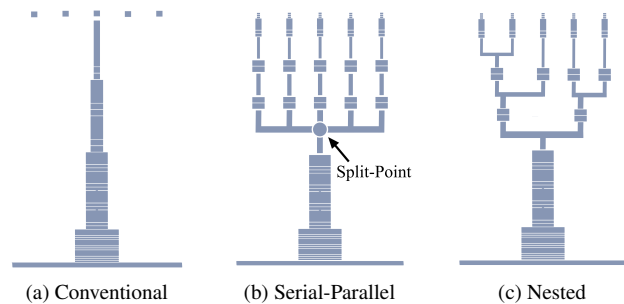


Figure 1. Neural network architectures. (a) conventional deep network from bottom to top (the dots represent five classes); (b) proposed serial-parallel hybrid: each class has its own branch; (c) proposed compromise between a and b with a nested structure.

shelf, the salt on the table, or our friend in a crowd, the human visual system is able to focus on target-relevant features and speed up processing considerably: Wolfe’s measurements of human visual perception show that the reaction speed of such a guided visual search is usually higher compared to an unguided search [44]. This aspect can also be observed across modalities. A recent neuroscience paper by Marian *et al.* [31] inspired this work, and argues that in the presence of audio signals such as a “meow,” which already allow semantic inferences about a searched object, humans can speed up their visual search and perceive the object more quickly, e.g., a “cat”. It is assumed that there is a contextual connection between modalities and thus, e.g., visual class-specific features for objects can be specifically activated. Even with the most advanced DL (Deep Learning) methods, such behavior cannot be easily reproduced [18]. So the question is: What would an artificial neural network have to look like to have that kind of acceleration capability?

We assume that we should be able to exclude irrelevant features from the process to reduce processing time. But DL methods are often described as black boxes [3], so even the

visualization of class-specific features is limited [35]. This property makes it challenging to use top-down cues, e.g. target or context information [4], which could be useful to focus on relevant features and speed up processing; instead, widely used attention mechanisms, such as for transformers, tend to be bottom-up, i.e. they focus on the given data [38]. This kind of attention is mainly statistically driven by many images or patches because these are needed for the mechanism to learn which features are more important than others for a particular decision. However, since we want to incorporate cues from the cognitive level ("meow" → "cat") that include or exclude certain object classes in processing, top-down attention is more appropriate for our purposes.

For these reasons, we restructure the standard architecture of deep networks to get access to high-level features that usually cannot be addressed directly using a context. Recent neuroscience studies show that layer 2 in primary visual cortex responds in a context-specific way through spatially separated neurons [29,45] -, similar to what we intend here: By parallelization of the layers towards the end of the network, features can be separated class-specifically [34]. They can now be amplified by simple scalar weighting, or processed by attention, while low and mid-level features can still be shared by all classes. Intuitively, this makes sense, because they are generic and useful for all categories. But for high-level features it makes less sense, because eyes are not useful for cars, for example. Figure 1 schematically shows the current convention (1a), the proposed structure (1b) and a nested structure (1c) as a compromise between the two. Our contributions are as follows:

- a novel serial-parallel hybrid for generating class-specific representations - similar to context-specific representations in the human brain [37].
- class-specific cutouts, consisting of the fixed serial part and the variable parallel part with class-specific features, that can be combined as desired. They allow a more adaptable model and lower inference costs.
- a built-in selective attention mechanism at the class-specific level enabling to actively influence the result of an image classification network

Overall, the serial-parallel hybrid generates class-specific high-level features [46] for another step towards interpretable AI, while providing the ability to bypass unneeded high-level features to reduce parameters, computational cost, and power consumption during inference. This is important for mobile computing, industrial, drone, or robotic applications [6, 7, 40, 42], and because the cost of inference and the cost of training for AI models used in industry is up to 9:1 [14].

2. Related Work

2.1. Image Classification

The good CV (Computer Vision) practice of training and validating on ImageNet for image classification is beginning to decline. Methods such as transformers [48], very large language models [5], knowledge distillation [8], wild and large datasets [30], unsupervised learning [9] and appropriate loss functions [41], etc., make the formerly state-of-the-art pre-training on ImageNet [22] to a downstream fine-training to visualize CV's advances by validation [47]. What remains almost the same, however, is the fact that at the time of inference, all high-level features must be processed, because all of them are included in the decision process, even if some of them are weighted with zero. This can be considered a large overhead, since the decision-relevant features change depending on the task and context. Adaptation could save parameters, energy, and processing time. This is where our method comes in, so that high-level features can be generated class-specifically through parallelization and excluded when not needed.

2.2. Bottom-up vs. Top-Down Attention

Selective attention is a mechanism of human perception that enables us to focus on regions of potential interest [11, 28]. These can be objects, colors, locations, sounds, or other patterns. It helps us to deal with the complexity of the world and quickly find objects of interest. Attention is driven by two types of cues: bottom-up and top-down cues [36]. Bottom-up cues are salient patterns that automatically attract attention, such as a red flower on green grass. Top-down attention, on the other hand, focuses on regions which are behaviorally relevant and is driven by pre-knowledge, goals, or expectations. Searching for our key, or the well-known cocktail-party effect [2] are examples of top-down attention.

During the last years, attention mechanisms became very popular in DL [12]. However, most of them cannot simply focus in a top-down manner like biological systems. They usually base their processing on the input data and do not consider pre-knowledge about the target or the scene. Early works before the DL era have amplified target-relevant features by excitation and inhibition of pre-computed features to realize top-down attention [17, 32]. In deep networks, top-down attention is usually understood as a tracing the activations backwards through the network from class nodes to the feature maps, as in GradCAM [35], and is often used to localize class-specific features in feature maps. However, this requires one forward-pass of the input image through the network, before the backward tracing can be performed, and does not enable a quicker processing through the usage of pre-knowledge as in human perception.

2.3. Parallel Branched Networks

One of the most cited DL methods that introduces useful branching is ResNet [20]. Skip connections parallel to information flow, allowing identity mapping and much deeper networks than before. To put it in a nutshell: There are parallel branches everywhere in the DL [19, 25, 39]!

But branching, as we introduce it here, is rarely used and is even unique in its degree of parallelization and in the context of selective attention. At first sight it reminds of ensemble learning, where multiple neural networks are trained side by side, e.g., to solve a task very precisely [1, 27], but it is different. There, often x different models are used, sometimes with y different types of input, while we train a single model with the same input type and k different branches. This model is characterized by its serial-parallel hybrid structure. Thus, low-level and mid-level features can still be shared by all classes, while high-level features are separated in a class-specific way. A work more related to ours than previously listed ones is the tree-like branching (TLB) network from Xue *et al.* [46] with a class-specific branching. They are building a tree structure based on the similarities of the categories and show improvements for image classification. Differences to ours are that they do not draw any parallels to brain inspiration or a relation to selective attention, and although they talk about improved inference time, they seem to mean the model as a whole and do not mention the novelty of inference cost reduction through cutouts introduced here.

3. Proposed Method

As mentioned earlier, a limitation of current DL methods is that they cannot be easily accelerated or focused like biological systems [31] when, for example, high-level knowledge is available from other modalities or insights. Due to their black-box properties [3], most models do not reveal where class-specific features are located in the deep network. To address this and the lack of possibilities for speedup, we rethink the conventional architecture and propose a serial-parallel hybrid system. Recent neuroscientific studies support our approach and show that the human brain also has context-specific areas [29, 45]. In Sec 3.1 the principle of the method is given and its variants are shown in detail. In Sec. 3.2, our approach is used to reduce inference costs and the loss function is given. The Sec. 3.3 contains how to nest high-level features to selectively share parameters.

3.1. High-Level Feature Parallelization

We are exploring a new architecture, whose principle can be applied to modern models. Therefore, we have based our model on a widely known standard, the ResNet50. Figure 2b shows our proposed HLFP network (High-Level

lay.\mod.	HLFP-small	HLFP-big	HLFP-late-SP	ResNet50
input	224 × 224 × 3			
conv 1	7 × 7 × 3 × 64, stride 2			
pool 1	3 × 3, max			
output	56 × 56			
conv 2a	1 × 1 × 64			
conv 2b	3 × 3 × 64			
conv 2c	1 × 1 × 64 × 64/256			
reps	3			
output	28 × 28			
conv 3a	1 × 1 × 256 × 128			
conv 3b	3 × 3 × 128 × 128			
conv 3c	1 × 1 × 128 × 128/512			
reps	4			
output	14 × 14			
conv 4a	1×1×512×128	1×1×512×256		
conv 4b	3×3×128×128	3×3×256×256		
conv 4c	1×1×128×512	1×1×256×256/1024		
reps	1	6		
PAR	k	1		
output	7×7			
conv 5a	1×1×512×64	1×1×1024×128	1×1×1024×512	
conv 5b	3×3×64×64	3×3×128×128	3×3×512×512	
conv 5c	1×1×64×256	1×1×128×512	1×1×256×512/2048	
reps	1			3
PAR	k	k	1	
output	3 × 3			
conv 6a	1×1×256×32	1×1×512×64		
conv 6b	3×3×32×32	3×3×64×64		
conv 6c	1×1×32×128	1×1×64×256		
reps	1			
output	1 × 1		3 × 3	
conv 7a			1×1×256×32	
conv 7b			3×3×32×32	
conv 7c			1×1×32×128	
reps	1			
PAR			k	
output	1 × 1		3 × 3	
pool&flat	3 × 3 average pooling + flatten layer			
FC	128	256	128	2048
output	1 × 1 × 1 × k			

Table 1. Detailed model architectures. Left: three variants of our HLFP network; right: a ResNet50 of conventional type. The red boxes indicate the location of the split-point that introduces the main change: HLFPs get as many parallel branches as the classes k to be recognized; ResNets have only one. On the other hand, HLFP has fewer conv blocks serial repetitions (abbreviated as reps) - resulting in a much shallower net. The blue box is the insertion point for a second hierarchy level for HLFP-nested.

Features Parallelization). We define it through multiple blocks which contain multiple layers. The HLFP can be divided into two parts: the first layers, which are classically serial, including ResNet skip connections, and the deeper layers, which have parallel information flow. In Table 1 we have listed three variants of HLFP. These differ by fewer (small) or more (big) channels per parallel branch or by a later split-point (late-SP). Another variant not listed here is the HLFP-late-big-SP (late big split-point), which has the same basic structure as the HLFP-late-SP, but its split-point has twice as many channels. The hypothesis behind splitting the architecture into multiple branches while simultaneously processing the initial input through a serial network is that lower-level features are generic and useful for almost

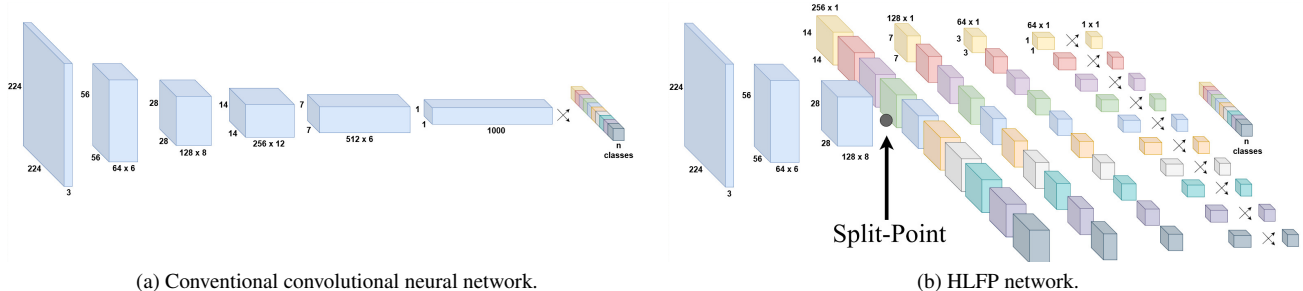


Figure 2. (a) shows the most common network architecture for vanilla classification networks, where data flow from layer to layer is mainly serial. (b) Our architecture also starts serially, but becomes parallel after a split-point to generate class-specific features spatially separated from each other. The different colors represent the classes and their branches. The resolution and the dimension of the feature channel, multiplied by the number of layers have exemplary values for a better understanding.

any class, while higher-level features are more specific, e.g., eye features are not required for a car and should therefore be treated in parallel. We define this connection as the split-point that connects the two parts of the network. Intuitively, a split-point could benefit from a larger number of parameters as it has to handle $1 : k$ connections, so we use a bottleneck structure [20].

Split-Point: Formally, we define the first part of our architecture to consist of shared network layers up to the split-point through the function: $\phi(x, \theta_0)$, taking the input image x and network parameters θ_0 as input. As we provide a branch for each of the target classes k , we define the number of final branches to be the same as our k target classes. Hence, we use $1 \leq i \leq k$ branch networks that we define through $\psi(\bar{x}, \theta_i)$, which take the output features of ϕ as input for \bar{x} . As all branch networks have the same design, we only exchange the network parameters θ_i for the classification of the i^{th} class. Using the above definitions allows us to define the output of the i^{th} branch network, which is responsible for class i , as:

$$f_i(x) = \psi(\phi(x, \theta_0), \theta_i) = y_i. \quad (1)$$

3.2. Cutouts

Conventional architectures usually do not have the ability to omit class-specific high-level features that are not needed. Often it is not even clear which parameter contributes to which class. However, if new information is available that simplifies the task, e.g. in image classification only 5 objects are relevant instead of 10, such an option to skip class-specific features would be advantageous. Through the above made definition of a split-point, we can define cutouts that allows the network to adapt to simpler tasks in the case that prior knowledge is available. This enables the formation of selected class-specific paths that are shorter and faster than if a standard neural network has to be used. Here, we extract $n \leq k$ selected

paths using a-priori knowledge of potential n new target classes $C = \{i_0, \dots, i_n \mid 1 \leq i_j \leq k\}$, while simultaneously keeping the branch fully functional. This allows us to define the probability of a sample belonging to that class $i \in C$ through:

$$p_i(x) = \frac{e^{-f_i(x)}}{\sum_{j \in C} e^{-f_j(x)}}. \quad (2)$$

The ability to adapt to the lower complexity of a task with less computational effort, but also to increase it when needed, is reminiscent of efficient and effective biological systems and their ability to focus.

Cross-Entropy Loss: For training of the network, we retain all initial target classes and estimate the class probability over all classes for the likelihood of an input x belonging to a class and utilized a cross-entropy as our loss function. Note also that this is the special case of Eq. 2 where we utilize all classes instead of a subset. The result of the likelihood estimation is included in a 1 vs. all classification and the cross entropy loss, see details in Figure 3. Optimizing the loss through backpropagation results in a high-value output for an image that belongs to the branch and a low-value output otherwise. Due to the softmax function, all paths are learned at once. Figure 3 illustrates this central point of our approach.

3.3. Nested Architecture

By pursuing the idea of class-dependent feature similarity and feature sharing at different hierarchical levels between image classes, we assume that a more optimal network architecture can be constructed by nesting branches depending on the categories and their superclasses. Figure 1c shows a schematic of such an architecture. We hypothesize that there are higher-level features that should be shared, such as wheels for buses and cars. To get an additional level of hierarchy, we use the superclasses provided

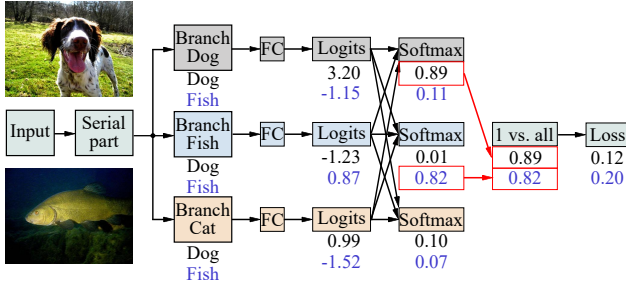


Figure 3. Three-branched HLFP network for dog, fish and cat classes with some example values (black: input dog, blue: input fish). The red boxes indicate the selection for 1 vs. all. Images from Imagenette [21].

by imagenet-superclass and Wordnet [15] is used to identify similarities between fine and coarse ImageNet classes [33] [13]. With this, we define this extended architecture by introducing another split-point, indicated by the blue box for HLFP-small in Table 1. Here, multiple branches i share the features of a superclass j through an additional network layer $\pi(\hat{x}, \hat{\theta}_j)$ with network parameters $\hat{\theta}$ and again taking the output of ϕ as input for \hat{x} and passing its output to \hat{x} of ψ . Hence, a total number of superclasses s results in an equal number of branches $1 \leq j \leq s$ in the lower hierarchical layer. Note that this does not change the total number of terminal branches k in the upper hierarchical layer, since they are still equal to the number of classes in the dataset. This allows us to redefine the output of the hierarchical branching network:

$$\hat{f}_i(x) = \psi(\pi(\phi(x, \theta_0), \hat{\theta}_j), \theta_i) = y_i. \quad (3)$$

To train the network, we use the aforementioned cross-entropy loss and our redefined softmax to still retain the possibility of cutouts on our nested architecture. However, we would like to note that when performing a cutout for a branch i it still requires the cutout network to retain the shared layer of its superclass j .

4. Experiments

We evaluate six different models: HLFP-small, -big (see Sec. 3.1), -nested (see Sec. 3.3), -late-SP (see Sec. 3.1), -1b-late-SP (one branch late Split-Point) and -late-big-SP (see Sec. 3.1). HLFP-1b-late-SP has not yet been introduced, but is nothing other than the model HLFP-late-SP with a single of the otherwise parallel branches. HLFP-attention (see Sec. 4.5) is not a separate model because it is an amplification of certain feature maps in the respective branches and can be applied to all HLFP networks. The ResNet50 [20] serves as the baseline, because it allows a direct comparison of the serial vs. serial-parallel structure, since the main building blocks for HLFP are the same. In order to capture lower and upper limits of performance, we have also added

a ResNet18 and 152. In Sec. 4.1 we provide some training information and introduce the datasets for our experiments. In Sec. 4.2, we test our approach for the image classification task, and in Sec. 4.3 we experiment on the reduction of inference costs with cutouts in terms of parameters, computational complexity and top-1 accuracy compared to standard methods. Sec. 4.4 illustrates and measures the potential for accelerated inference times and in Sec. 4.5 we take advantage of the built-in selective attention mechanism.

4.1. Training and Datasets

We have implemented all models in the Timm library [43] and used Rand Augment [10]. We have three different levels of classification complexity and training setups for studying HLFP:

- 10 classes with 1000 epochs, batch size 32
- 100 classes with 300 epochs, batch size 56, maxed out 24, 564 MebiBytes (MiB), mixed precision training
- 1000 classes with 300 epochs and batch size 24, and another run with batch size 46, maxed out 24, 564 and 49, 140 MiB, both trained through mixed precision training

As datasets, we chose subsets of ImageNet [13]. Imagenette and Imagewoof [21] both contain 10 classes, with the interesting property that Imagenette contains classes, which differ considerably, and Imagewoof has quite similar classes (breeds of dogs). Testing these two datasets helps to understand how the parallel branches handle similar and dissimilar classes. ImageNet100 [13] has some similar and some different classes, but shows if the model can handle a factor of 10 upscaling. The datasets used here have similar class and image numbers, and therefore a similar significance to Cifar10 and -100. These are not used because their lower image resolution would introduce an unwanted new factor into the evaluation [23, 24]. We were unable to test the model’s performance on ImageNet1k due to several months of training time. ImageNet mini [16] is a subset of this and has only a few images per class, about 20-50, but offers a high classification complexity with 1000 classes. We evaluate the top-1 accuracy and omit the top-5, as this is not very meaningful for the datasets with few classes.

4.2. Image Classification

For 10 classes the HLFP nets have a top-1 acc. comparable to the ResNets. This can be seen in Table 2. The HLFP-late-SP performs even better than the baseline with fewer parameters. When scaling the HLFP to 100 classes, the performance remains at a high level, but usually is a little below the baseline. HLFP-small performs as well as HLFP-big, despite significantly fewer parameters, suggesting that HLFP-big may be oversized. The split-point may no longer

model \dataset	no. parameter 10 classes	Imagenette top-1 acc.	Imagewoof top-1 acc.	no. parameter 100 classes	ImageNet100 top-1 acc.	no. parameter 1000 classes	ImageNet mini top-1 acc.
ResNet152	58,164,298	96.33	90.89	58,348,708	86.24	60,192,808	31.12
ResNet18	11,181,642	95.52	89.97	11,227,812	81.76	11,689,512	28.52
ResNet50 baseline	23,528,522	96.15	90.30	23,712,932	85.34	25,557,032	33.38
HLFP-big	27,464,778	95.75	90.02	261,643,428	82.26	2,603,429,928	***
HLFP-small	9,611,338	95.71	89.97	83,109,028	82.52	818,213,928	21.10
HLFP-nested	-	-	-	65,725,604	84.02	577,977,384	19.98
HLFP-late-SP	19,986,506	96.28	90.86	122,975,396	84.49	1,152,864,296	20.57
HLFP-1b-late-SP	9,688,778	95.90	90.61	9,700,388	83.94	9,816,488	30.49
HLFP-late-big-SP	-	-	-	348,643,492	85.80	-	***
HLFP-attention	9,611,338	+0.67	+0.56	83,109,028	+0.04	818,213,928	+0.24

Table 2. Image classification results on different datasets of ResNets and our HLFP variants including neural network parameters. Best values in bold for ResNet50 baseline, *** marks computationally too costly. Entries that are not evaluated are marked with -. Attention is applied to HLFP-small (see Sec. 4.5), resulting in a top-1 acc. gain shown in the bottom line.

accurately handle 1 : k connections. HLFP-nested relax this ratio and show a better result than the HLFP-small, although some superclasses are allowed to collect up to 7 fine classes and other superclasses have only one fine class, causing an imbalance that the model has to handle. This time, only the HLFP-late-big-SP with the extra channels added for the split-point can beat the baseline. In the 1000 classes, HPFL is not able to show a better performance than the baseline. The ResNet152 also shows for the first time a loss of acc. compared to the Resnet50. We assume that too many parameters are critical for ImageNet mini - especially because of the small number of images per class. This makes the stability of the HLFP remarkable for parameters up to the billion range. It is worth noting that parallelization gives HLFP an acc. advantage, as shown by comparing a single-branch HLFP-1b-late-SP model with HLFP-late-SP for all datasets (except ImageNet mini).

4.3. Inference Cost Reduction

The cutouts presented in Sec. 3.1 are a unique property of HLFP, where parameters are reduced by focusing only on the remaining and relevant classes, adapting to a changing task without requiring retraining. For the evaluation, we have divided the datasets into two subsets: lower label classes (e.g., class-ID: 1-5) and upper label classes (e.g., class-ID: 6-10). To start somewhere, we divide the 10 classes 50:50 and the 100 classes 80:20. For the baseline, we have ResNets that are trained like the cutouts on the full dataset and validated only on the subset, and ResNets that are completely new trained only on the subset. For Imagenette upper and lower 5 the cutouts have a better top-1 acc. than newly trained ResNets, visible in Table 3. Slightly better are the ResNets, also trained on 10 classes, but the cutouts are able to reduce the parameters by more than 75%. To determine the computational complexity, we count multiply-accumulate operations (MACs) and find that

model	ResNet50		HLFP-cutout	
dataset	Imagenette			
GMACs	4.13		2.66	
parameter	23,518,277	23,528,522	5,528,133	
train	upper 5	all 10	all 10	
val	upper 5	upper 5	upper 5	
top-1 acc.	97.16	97.83	97.62	
train	lower 5	all 10	all 10	
val	lower 5	lower 5	lower 5	
top-1 acc.	96.79	98.04	97.09	
dataset	Imagewoof			
train	upper 5	all 10	all 10	
val	upper 5	upper 5	upper 5	
top-1 acc.	91.18	91.88	91.34	
train	lower 5	all 10	all 10	
val	lower 5	lower 5	lower 5	
top-1 acc.	96.23	94.30	95.02	
model	ResNet50		HLFP-cutout	HLFP-nested
dataset	ImageNet100			
GMACs	4.13		14.85	10.79
parameter	23,671,952	23,712,932	66,776,208	51,565,712
train	upper 80	all 100	all 100	all 100
val	upper 80	upper 80	upper 80	upper 80
top-1 acc.	84.78	84.45	81.98	83.63
GMACs	4.13		6.72	4.66
parameter	23,549,012	23,712,932	17,777,748	16,148,052
train	lower 20	all 100	all 100	all 100
val	lower 20	lower 20	lower 20	lower 20
top-1 acc.	88.50	90.60	90.60	89.70

Table 3. Comparison of the inference costs of ResNet50 and the cutout of HLFP-small. The datasets are divided into two subsets: the upper one (the first x classes) and the lower one (the remaining y classes).

we can save about 35% while maintaining very high performance. In Imagewoof, the cutouts have a top-1 acc. with similarly high values for the upper and lower 5, and again with the same high reduction of parameters and MACs. ImageNet100 is divided into two different sizes: upper 80 and lower 20 classes. For the upper 80, the top-1 acc. of the relatively larger cutout has many more parameters and the

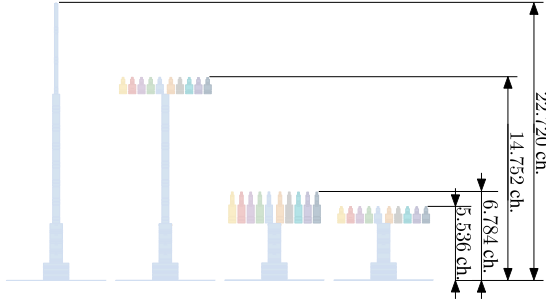


Figure 4. Depth visualization (almost to scale) of ResNet50, HLFP-late-SP, big and small, from left to right in that order. Further to the right is the sum of all channels for each net.

inference \ model variant	ResNet50	HLFP (one branch)		
		late-SP	big	small
time [ms]	8.4	8.0	5.5	5.3

Table 4. Inference time of ResNet50 and HLFP (theoretically with parallel processing).

top-1 acc. is not as good as the baselines. However, for the lower 20, the cutout has the best result with the ResNet trained on all classes, but with a reduction of about 6 million parameters.

4.4. Accelerated Inference

Our approach provides the ability to accelerate processes through parallel processing. In Fig. 4, all feature channels of the conventional ResNet50 are drawn almost to scale next to the HLFPs. In theory, the high-level features, which are clearly visible due to their multiple colors, can be processed in parallel. This is currently not possible with conventional models, such as the one in Fig. 1a, where each layer usually builds on the output of the previous one. In Table 4 we measure the inference time for ResNet and the theoretical one for HLFP by reducing its variants to a single branch. This illustrates the potential for HLFP to reduce inference time. For a more realistic time measurement, the CPU and GPU are synchronized and the GPU is warmed up.

4.5. Built-in Selective Attention

Consider a task where objects shall be classified in images and other modalities such as audio or descriptions are already available and provide semantic prior knowledge. This leads to contextual cues that can positively influence the classification, e.g. a "meow" should strengthen the classification of the object "cat" as in human perception [44].

We argue that the proposed HLFP has a built-in selective attention mechanism because we know where to access the class-specific high-level features, since individual feature maps can be associated with a branch, its parameters, and

a class. Figure 5 visualizes the feature maps of two parallel branches and shows class-specific differences. In an initial test, we assume that meaningful semantic knowledge already exists for each validation image, so that amplification should be done for each image class. This is done by simply multiplying the feature maps in the corresponding path in conv block 5 of HLFP-small (see Table 1) by a scalar, which is determined by experimentation. We use here values of 1.8 (Imagenette), 1.4 (Imagewoof), 1.1 (ImageNet100) and 1.3 (ImageNet mini). For the evaluation, the labels are used in such a way that a guidance exists that allows to find only the class-specific path of the respective validation image and to multiply the class-specific feature map from the conv block 5 with the scalar. This is done for all validation images and the last line in Table 2 shows that the classification result of HLFP-small is positively influenced. It is worth noting that this can be applied to any HLFP network. This novel built-in top-down attention should be further explored, as it is not available in conventional architectures without much more complex operations [26].

5. Conclusion

We introduce a novel approach, HLFP, for High-Level Feature Parallelization to reduce inference costs through selective attention. It's inspired by two recent neuroscientific studies: In particular, that semantic prior knowledge from another modality, here audio, accelerates visual processing through contextual connections; and that the human brain appears to contain spatially separated context-specific neural activations. Both observations are not common for deep networks, so we rethink the conventional architecture and implement a serial-parallel hybrid system based on ResNet50 for exemplary testing. Since this is a basic principle, it should be possible to apply it to the latest, already effective and/or unsupervised methods. The conventional network remains up to a certain point, the split point, and then a grouped convolution, performed once, forms individual branches that are responsible for and assigned to the classification of a class. We see two ways in which HLFP can reduce inference costs. First, by being more parallel and less deep, the network becomes shallower, so parallel processing could theoretically reduce inference time. Second, we introduce cutouts, a unique feature of HLFP where parameters are reduced by focusing only on the remaining and relevant classes, adapting to a changing task without the need for retraining. We show examples where the number of parameters can be reduced by 75% and 35% fewer GMACs can be used by adapting to a new task, but the high performance remains almost the same.

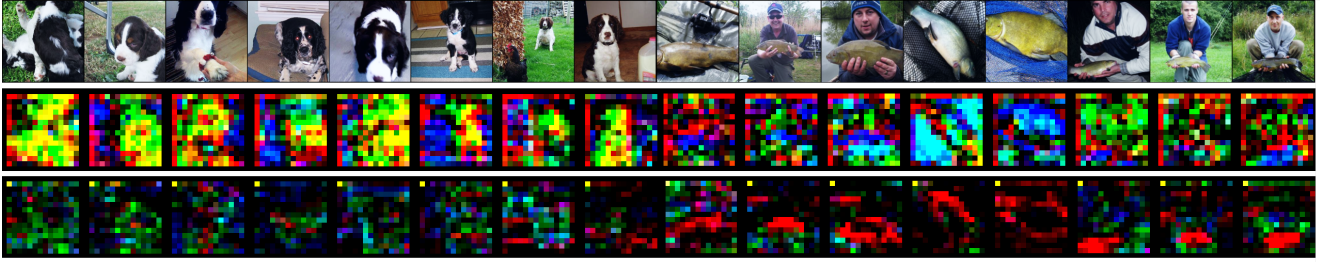


Figure 5. Original images from Imagenette [21] and class-specific features. The first row shows the original images at reduced resolution. The second and third rows show $14 \times 14 \times 3$ RGB-colored class-specific high-level features from HLFP-big - conv 4, where the upper ones were extracted from the "Dog" branch and the lower ones from the "Fish" branch. The selected feature maps from the Dog branch are salient for the Dog object and less salient for the Fish object. The opposite is observed for the Fish branch.

References

- [1] Sanghyeon An, Min Jun Lee, Sanglee Park, He Sarina Yang, and Jungmin So. An ensemble of simple convolutional neural network models for mnist digit recognition. *ArXiv*, abs/2008.10400, 2020. 3
- [2] Barry Arons. A review of the cocktail party effect. *Journal of the American Voice I/O Society*, 12(7):35–50, 1992. 2
- [3] Caglar Aytekin. Neural networks are decision trees. *ArXiv*, abs/2210.05189, 2022. 1, 3
- [4] Soubarna Banik, Mikko Lauri, Alois Knoll, and Simone Frintrop. Object localization with attribute preference based on top-down attention. In Markus Vincze, Timothy Patten, Henrik I. Christensen, Lazaros Nalpantidis, and Ming Liu, editors, *Computer Vision Systems*, pages 28–40, Cham, 2021. Springer International Publishing. 2
- [5] Tom Brown, Benjamin Mann, Nick Ryder, Melanie Subbiah, Jared D Kaplan, Prafulla Dhariwal, Arvind Neelakantan, Pranav Shyam, Girish Sastry, Amanda Askell, Sandhini Agarwal, Ariel Herbert-Voss, Gretchen Krueger, Tom Henighan, Rewon Child, Aditya Ramesh, Daniel Ziegler, Jeffrey Wu, Clemens Winter, Chris Hesse, Mark Chen, Eric Sigler, Matusz Litwin, Scott Gray, Benjamin Chess, Jack Clark, Christopher Berner, Sam McCandlish, Alec Radford, Ilya Sutskever, and Dario Amodei. Language models are few-shot learners. In H. Larochelle, M. Ranzato, R. Hadsell, M.F. Balcan, and H. Lin, editors, *Advances in Neural Information Processing Systems*, volume 33, pages 1877–1901. Curran Associates, Inc., 2020. 2
- [6] Widodo Budiharto, Alexander A S Gunawan, Jarot S. Suroso, Andry Chowanda, Aurello Patrik, and Gaudi Utama. Fast object detection for quadcopter drone using deep learning. In *2018 3rd International Conference on Computer and Communication Systems (ICCCS)*, pages 192–195, 2018. 2
- [7] Han Cai, Ji Lin, Yujun Lin, Zhijian Liu, Haotian Tang, Hanrui Wang, Ligeng Zhu, and Song Han. Enable deep learning on mobile devices: Methods, systems, and applications. *ACM Trans. Des. Autom. Electron. Syst.*, 27(3), mar 2022. 2
- [8] Mathilde Caron, Hugo Touvron, Ishan Misra, Hervé Jegou, Julien Mairal, Piotr Bojanowski, and Armand Joulin. Emerging properties in self-supervised vision transformers. In *2021 IEEE/CVF International Conference on Computer Vision (ICCV)*, pages 9630–9640, 2021. 2
- [9] Ting Chen, Simon Kornblith, Mohammad Norouzi, and Geoffrey Hinton. A simple framework for contrastive learning of visual representations. In *Proceedings of the 37th International Conference on Machine Learning, ICML'20*. JMLR.org, 2020. 2
- [10] Ekin D. Cubuk, Barret Zoph, Jonathon Shlens, and Quoc V. Le. Randaugment: Practical automated data augmentation with a reduced search space. In *2020 IEEE/CVF Conference on Computer Vision and Pattern Recognition Workshops (CVPRW)*, pages 3008–3017, 2020. 5
- [11] Elizabeth T Davis and John Palmer. Visual search and attention: an overview. *Spatial Vision*, 2004. 2
- [12] Alana de Santana Correia and E. Colombini. Attention, please! a survey of neural attention models in deep learning. *Artificial Intelligence Review*, 55:6037 – 6124, 2022. 2
- [13] Jia Deng, Wei Dong, Richard Socher, Li-Jia Li, Kai Li, and Li Fei-Fei. Imagenet: A large-scale hierarchical image database. In *2009 IEEE conference on computer vision and pattern recognition*, pages 248–255. Ieee, 2009. 5
- [14] Radosvet Desislavov, Fernando Martínez-Plumed, and José Hernández-Orallo. Trends in ai inference energy consumption: Beyond the performance-vs-parameter laws of deep learning. *Sustainable Computing: Informatics and Systems*, 38:100857, 2023. 2
- [15] Christiane Fellbaum. *WordNet: An Electronic Lexical Database*. Bradford Books, 1998. 5
- [16] Ilya Figotin. Imagenet 1000 (mini). <https://www.kaggle.com/datasets/ifigotin/imagenetmini-1000>, Mar 2020. 5
- [17] Simone Frintrop, Gerriet Backer, and Erich Rome. Goal-directed search with a top-down modulated computational attention system. In *Pattern Recognition: 27th DAGM Symposium, Vienna, Austria, August 31-September 2, 2005. Proceedings 27*, pages 117–124. Springer, 2005. 2
- [18] Di Fu, Cornelius Weber, Guochun Yang, Matthias Kerzel, Weizhi Nan, Pablo Barros, Haiyan Wu, Xun Liu, and Stefan Wermter. What can computational models learn from human selective attention? a review from an audiovisual unimodal and crossmodal perspective. *Frontiers in Integrative Neuroscience*, 14, 2020. 1

- [19] Ankit Goyal, Alexey Bochkovskiy, Jia Deng, and Vladlen Koltun. Non-deep networks, 2022. 3
- [20] K. He, X. Zhang, S. Ren, and J. Sun. Deep residual learning for image recognition. In *2016 IEEE Conference on Computer Vision and Pattern Recognition (CVPR)*, pages 770–778, June 2016. 3, 4, 5
- [21] Jeremy Howard. Imagenet. <https://github.com/fastai/imagenette/>. 5, 8
- [22] André Peter Kelm, Vijesh Soorya Rao, and Udo Zölzer. Object contour and edge detection with refinecontournet. In Mario Vento and Gennaro Percannella, editors, *Computer Analysis of Images and Patterns*, pages 246–258, Cham, 2019. Springer International Publishing. 2
- [23] Alex Krizhevsky, Vinod Nair, and Geoffrey Hinton. Cifar-10 (canadian institute for advanced research). 5
- [24] Alex Krizhevsky, Vinod Nair, and Geoffrey Hinton. Cifar-100 (canadian institute for advanced research). 5
- [25] Alex Krizhevsky, Ilya Sutskever, and Geoffrey E Hinton. Imagenet classification with deep convolutional neural networks. In F. Pereira, C. J. C. Burges, L. Bottou, and K. Q. Weinberger, editors, *Advances in Neural Information Processing Systems 25*, pages 1097–1105. Curran Associates, Inc., 2012. 3
- [26] Ting-Yu Kuo, Yuanda Liao, Kai Li, Bo Hong, and Xiaolin Hu. Inferring mechanisms of auditory attentional modulation with deep neural networks. *Neural Computation*, 34(11):2273–2293, 2022. 7
- [27] Retno Larasati and Hak KeungLam. Handwritten digits recognition using ensemble neural networks and ensemble decision tree. In *2017 International Conference on Smart Cities, Automation & Intelligent Computing Systems (ICONSONICS)*, pages 99–104, 2017. 3
- [28] Tidhar Lev-Ari, Hadar Beerli, and Yoram Gutfreund. The ecological view of selective attention. *Frontiers in Integrative Neuroscience*, 16, 2022. 2
- [29] Kai-Yuan Liu, Xing-Yu Li, Yu-Rui Lai, Hang Su, Jia-Chen Wang, Chun-Xu Guo, Hong Xie, Ji-Song Guan, and Yi Zhou. Denoised internal models: A brain-inspired autoencoder against adversarial attacks. *Machine Intelligence Research*, 19(5):456–471, Oct 2022. 2, 3
- [30] Dhruv Mahajan, Ross Girshick, Vignesh Ramanathan, Kaiming He, Manohar Paluri, Yixuan Li, Ashwin Bharambe, and Laurens van der Maaten. Exploring the limits of weakly supervised pretraining. In *Computer Vision – ECCV 2018: 15th European Conference, Munich, Germany, September 8-14, 2018, Proceedings, Part II*, page 185–201, Berlin, Heidelberg, 2018. Springer-Verlag. 2
- [31] Viorica Marian, Sayuri Hayakawa, and Scott R. Schroeder. Cross-modal interaction between auditory and visual input impacts memory retrieval. *Frontiers in Neuroscience*, 15, 2021. 1, 3
- [32] Vidhya Navalpakkam and Laurent Itti. Modeling the influence of task on attention. *Vision research*, 45(2):205–231, 2005. 2
- [33] S-Kumano. S-kumano/imagenet-superclass: The example of correspondence between fine classes and superclass (coarse class) in imagenet. <https://github.com/s-kumano/imagenet-superclass>. 5
- [34] Ali Sekmen, Mustafa Parlaktuna, Ayad Abdul-Malek, Erdem Erdemir, and Ahmet Buğra Koku. Robust feature space separation for deep convolutional neural network training. *Discover Artificial Intelligence*, 1(12):1–11, 2021. 2
- [35] Ramprasaath R Selvaraju, Michael Cogswell, Abhishek Das, Ramakrishna Vedantam, Devi Parikh, and Dhruv Batra. Grad-cam: Visual explanations from deep networks via gradient-based localization. In *Proceedings of the IEEE international conference on computer vision*, pages 618–626, 2017. 2
- [36] Jan Theeuwes. Top-down and bottom-up control of visual selection. *Acta psychologica*, 135(2):77–99, 2010. 2
- [37] Susumu Tonegawa, Xu Liu, Steve Ramirez, and Roger Redondo. Memory engram cells have come of age. *Neuron*, 87(5):918–931, 2015. 2
- [38] Ashish Vaswani, Noam Shazeer, Niki Parmar, Jakob Uszkoreit, Llion Jones, Aidan N Gomez, Łukasz Kaiser, and Illia Polosukhin. Attention is all you need. In I. Guyon, U. Von Luxburg, S. Bengio, H. Wallach, R. Fergus, S. Vishwanathan, and R. Garnett, editors, *Advances in Neural Information Processing Systems*, volume 30. Curran Associates, Inc., 2017. 2
- [39] Matthew Wallingford, Hao Li, Alessandro Achille, Avinash Ravichandran, Charles Fowlkes, Rahul Bhotika, and Stefano Soatto. Task adaptive parameter sharing for multi-task learning. In *Proceedings of the IEEE/CVF Conference on Computer Vision and Pattern Recognition (CVPR)*, pages 7561–7570, June 2022. 3
- [40] Ji Wang, Bokai Cao, Philip Yu, Lichao Sun, Weidong Bao, and Xiaomin Zhu. Deep learning towards mobile applications. In *2018 IEEE 38th International Conference on Distributed Computing Systems (ICDCS)*, pages 1385–1393, 2018. 2
- [41] Yisen Wang, Xingjun Ma, Zaiyi Chen, Yuan Luo, Jinfeng Yi, and James Bailey. Symmetric cross entropy for robust learning with noisy labels. In *2019 IEEE/CVF International Conference on Computer Vision (ICCV)*, pages 322–330, 2019. 2
- [42] Yingchun Wang, Jingyi Wang, Weizhan Zhang, Yufeng Zhan, Song Guo, Qinghua Zheng, and Xuanyu Wang. A survey on deploying mobile deep learning applications: A systemic and technical perspective. *Digital Communications and Networks*, 8(1):1–17, 2022. 2
- [43] Ross Wightman. Pytorch image models. <https://github.com/rwightman/pytorch-image-models>, 2019. 5
- [44] Jeremy M. Wolfe. Guided search 6.0: An updated model of visual search. *Psychonomic Bulletin & Review*, 28(4):1060–1092, Aug 2021. 1, 7
- [45] Hong Xie, Yu Liu, Youzhi Zhu, Xinlu Ding, Yuhao Yang, and Ji-Song Guan. In vivo imaging of immediate early gene expression reveals layer-specific memory traces in the mammalian brain. *Proceedings of the National Academy of Sciences*, 111(7):2788–2793, 2014. 2, 3
- [46] Mengqi Xue, Jie Song, Li Sun, and Mingli Song. Tree-like branching network for multi-class classification. In Pandian Vasant, Ivan Zelinka, and Gerhard-Wilhelm Weber, edi-

- tors, *Intelligent Computing & Optimization*, pages 175–184, Cham, 2022. Springer International Publishing. 2, 3
- [47] Jiahui Yu, Zirui Wang, Vijay Vasudevan, Legg Yeung, Mojtaba Seyedhosseini, and Yonghui Wu. Coca: Contrastive captioners are image-text foundation models, 2022. 2
- [48] Zizhao Zhang, Han Zhang, Long Zhao, Ting Chen, Serkan Ö. Arik, and Tomas Pfister. Nested hierarchical transformer: Towards accurate, data-efficient and interpretable visual understanding. In *AAAI Conference on Artificial Intelligence*, 2021. 2